

REMOVAL OF BRILLIANT GREEN DYE FROM SIMULATED WASTEWATER USING KERATIN DERIVED FROM CHICKEN FEATHERS

Abstract

In this study, keratin chicken feathers (K-CF), which are keratin synthesized from waste chicken feathers, were used as an adsorbent in the sorption process for brilliant green dye removal from the wastewater. The keratin was synthesized by alkaline and acidic hydrolysis of keratin from chicken feathers. Factors affecting the adsorption process including dosage, contact time, initial dye concentration, and temperature, were investigated using batch adsorption process. The percentage removal of the BGD using K-CF was 98.0% at optimal conditions of pH 8, 0.09g/20ml and 40°. The equilibrium data were analyzed using Langmuir, Freundlich, Temkin, and Halsey isotherm models. The Langmuir isotherm model was the best fit, and the maximum adsorption capacity values were 81.3, 65.36, and 454.55 mg/g at 30°, 40°, and 50°C, respectively. The adsorption kinetic data corresponded to the pseudo-second-order model at all temperatures. Also, the Thermodynamic parameters, such as ΔG , ΔH , and ΔS were calculated and the results at optimal temperature of 40° were $-1,268,131\text{KJmol}^{-1}$, -11.508KJmol^{-1} and 4051.5KJmol^{-1} respectively confirming that the adsorptive process is feasible, spontaneous and exothermic in nature. Experimental results showed that the adsorption capacity increased with temperature and the K-CF was an effective adsorbent for removing brilliant green dye.

Keywords: Kratin Chicken Feathers, Adsorption, Brilliant Green Dye, Effluent, Equilibrium.

1. Introduction

“Globally, there have been clear indicators of substantial changes in the climate pattern of the planet due to excessive, uncultured, and unregulated industrial and individual activities with undeniable adverse environmental and climatic effects. For instance, the increasing concentration of emerging contaminants in water bodies universally is one of the greatest threats of the time. Industries like the textile industry consume a large amount of water and generate almost 90% of

wastewater” (Mondal *et al*, 2017). “Different types of dyes are being used by textile industries for coloring fabrics in large numbers, which are disposed into water bodies”[33,34,35].

“Color removal from these textile effluents has been the target of great attention in the last few years, not only because of their potential toxicity but largely due to their visibility problems. Continual dumping of these dye-contaminated wastewater from textile industries to the environment pollutes freshwater resources, thus, posing hazardous effects on the ecosystem and human beings”(Saravanan *et al*, 2014). “Moreover, dyes are toxic, and carcinogenic and lead to mutagenic problems” (Gupta *et al*, 2016). “Synthetic dyes have complex aromatic structures and they are ineffective upon exposure to light, heat, microbial attacks, or chemicals like oxidizing agents” (Nekouei *et al*, 2015; Bharathi and Ramesh, 2013). “Based on the structure and properties, dyes may be categorized as cationic (basic dye), anionic (direct, reactive, acid dyes), and non-ionic (dispersive dyes). Cationic dyes are generally brighter in color and more toxic than anionic dyes” (Etim *et al*, 2016).

“Brilliant green (BGD) (Figure 1) is a cationic dye that is an odorless yellow-green to green powder used for various purposes, including as a biological stain and dermatological agent, in veterinary medicine, and as an additive to poultry feed to inhibit the propagation of mold, intestinal parasites, and fungus. It is also extensively used in textile dyeing and paper printing” (Mane and Babu, 2011). “It has also been discovered that BGD is an irritant, causing skin and eye burns, nausea, vomiting, diarrhea, and abdominal pain; it is classified as very toxic, with a probable lethal dose of 50-500 mg/kg in humans” (Tavlieva *et al*, 2013).

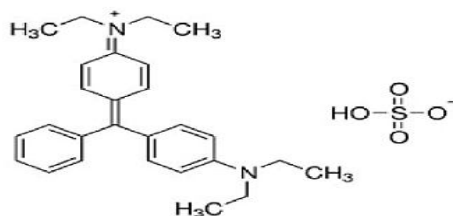


Fig.1 Structural Formular of BGD

Many techniques have been employed in the treatment of these effluents including photodegradation, heterogeneous catalytic discoloration, electrocoagulation, photovoltaic electrocoagulation process, catalytic oxidation, electrochemical degradation (Guenfoud et al., 2014), etc for dye removal, however, studies have shown that an adsorption is an efficient option for removing dyes from water and wastewater (Daneshvar et al., 2014). Besides, adsorption is environmentally friendly, cost-effective, and can give near-complete removal of the dyes (Onu et al. 2020a). In this study, keratin extracted from chicken feathers (K-CF) was employed to study the removal of brilliant green dye (BGD) contaminated textile wastewater. Chicken feathers, a significant part of the poultry industry's waste product, possess a robust protein structure composed mainly of keratin. Keratin is a biopolymer with unique properties, including high nitrogen content and slow degradation, presenting a good material for various applications in agriculture and other fields as well as other industrial applications like sorption processes because of its porosity and functional group contents.

Also, Keratin is a complex mixture of filament-forming proteins (Tinoco et al., 2020), it is characterized by a high content of sulfur-containing amino acids and is organized in two types of secondary structures, α -helix (e.g., wool) and β -sheet (e.g., feathers) (Chilakamarry et al., 2021). “The keratin chains are cross-linked by di-sulfuric bridges, which stabilize and rigidize the secondary and tertiary structures. Due to its complex and highly organized structures, keratin is insoluble in most of the known protein solvents and is resistant to the hydrolysis of the usual proteases, such as subtilisin, pepsin, papain, or trypsin” (Chaitanya et al., 2021).

“As a result of the complex and highly organized structure of keratin, the disposal of keratin-rich material is difficult. Landfilling generates high epidemiological risks, due to the proliferation of the keratinolytic (human) pathogens” (Duan et al., 2020). “Studies have shown that incineration raises technical difficulties due to the low flammability of keratin and produces hazardous substances like sulfur oxides” (Ossai et al., 2022). “The ideal solution for keratin is to use the high protein content of keratin-rich side streams for various applications - in food and feed industries or as agricultural inputs” (Alvarez-Castillo et al., 2021; Giteru et al., 2023; Perça-Crişan et al., 2021).

2. Materials and Methods

2.1. Materials and Chemicals Used

The Brilliant Green Dye (BGD) and other chemicals such as HCl, NaOH, pH 7.0 buffer tablets, and distilled water of analytical grades were sourced from a chemical vendor at Bridge Head, Onitsha, Anambra state, Nigeria. Modified Keratin chicken feathers (K-CF) were the adsorbent synthesized and used in the adsorption study. HCl and NaOH were used to adjust the pH of the solution, which was measured using a pH meter (PHS-25).

2.2 Methods

Using the modified synthesis of keratin from chicken feathers presented by Faraon et al, 2023, the collected chicken feathers were thoroughly washed with distilled water, sun-dried, and further oven dried at the temperature of 105°C for about 1 hour 30mins, and crushed. The ground chicken feather was hydrolyzed by mixing 0.5M solution of NaOH in 1L of flask with 25g of prepared ground chicken feather and the mixture was heated at 45°C at pH 10 for 5 hours with constant stirring on a hot plate. The mixture was allowed to cool to room temperature, and the solution was centrifuged at 10,000rpm for 5 mins. The supernatant liquid was collected and separated using filter paper. 100ml of 2N HCl solution was prepared and added dropwise to the filtrate collected in the ratio of 1:1 to crystalize the keratin in the hydrolyzed chicken feather solution. The crystals are separated from the solution by decanting and washed in 100 distilled water using a glass rod 5 to 6 times until the pH is neutral. The washed crystals were oven-dried at 50°C for 3 to 6 hours to get dry solids and ground to powder using a clean porcelain dish and stored in a clean bottle for use.

2.3. Adsorption Study

To study the effects of pH, adsorbent dosage, contaminant concentration, time, and temperature on the sorption process, experiments were carried out in batch modes using the modified procedure according to Okoye et al., (2019). The sorption experiments were evaluated in aqueous solutions containing 20ml of BGD and placed on a magnetic stirrer. The steps for the sorption experiment are as follows:

1. Some different 50 ml Pyrex beakers containing 20 ml of specified BGD concentration in five ranges and specified dosages of K-CF were set at different temperatures of 30°C, 40°C, 50°C, 60°C, and 70°C.
2. The beakers containing the mixtures were stirred using a magnetic stirrer at a speed of 110 rev/min for 150 min.
3. At the end of the set time for the treatment, the mixture was filtered using Whatman No. 1 filter paper.
4. After setting the absorbance-concentration profile, BGD concentrations were measured by UV spectrophotometric method at determined λ_{max} ($\lambda_{max-BGD} = 625 \text{ nm}$) (Wang *et al.*, 2015).

The effect of the variables such as contaminant concentration (BGD: 10, 20, 30, 40, 50mg/L), pH (2, 4, 6, 8, 10), contact time (10 - 180 min), adsorbent dose (0.03 – 0.15g/l) and temperature (30 - 70°C) were evaluated on the sorption experiments. The adsorption capacity of contaminants at the time, t (q_t (mg/g)) and equilibrium (q_e (mg/g)) was be calculated by the following formula (Khan *et al.*, 2021):

$$q_t = \frac{C_0 - C_t}{C_0} * 100 \quad (1)$$

$$q_e = \frac{(C_0 - C_e) * V}{m} \quad (2)$$

where C_0 , C_e , and C_t (mg/L) are model contaminant concentrations at the initial and equilibrium stages, and time t , respectively. The adsorbent mass is m (g), and V (L) represents the model contaminant solution volume. The removal efficiency was calculated as follows (Wang *et al.*, 2020b):

$$\text{Removal efficiency (\%)} = \frac{C_0 - C_e}{C_0} * 100 \quad (3)$$

2.4 Adsorption Kinetics Studies

The solute uptake rate is evaluated by an adsorptive kinetics study. The rate at which the dye ions will be adsorbed by the adsorbent will be studied at varying temperatures (30, 40, and 50°C). The pH of the adsorbate was adjusted to 8 and 40mg/L concentration in a batch-wise experiment was carried out. At a definite time of about 180 min, about 6ml of the solution was

withdrawn. The withdrawn solution was filtered and the concentration of the supernatant solution was measured and recorded. Pseudo-first-order, pseudo-second-order, Elovich model, Weber-Morris kinetic model, and Intra-particle diffusion model were all employed to describe rates of the sorption of the BGD by K-CF

According to Lagergren, the pseudo-first-order kinetic model equations can be expressed as follows (Bellir et al., 2010)

$$\frac{dq_t}{dt} = K_1(q_e - q_t) \quad (4)$$

where k_1 is the rate constant of the model, it is the amount of solute adsorbed on the adsorbent at time t , and q_e is the amount at equilibrium. Integrating and applying boundary conditions $q_t = 0$ at $t = 0$ and $q_t = q_t$ at $t = t$, the natural logarithmic form of Eq. (4) was obtained:

$$\ln(q_e - q_t) = \ln q_e - K_1 t \quad (5)$$

Rearranging Eq. (5), the nonlinear form of the pseudo-first-order kinetic equation is stated as:

$$q_t = q_e(1 - e^{-K_1 t}) \quad (6)$$

Also, the non-linear pseudo-second-order kinetic model equation is expressed as:

$$q_t = \frac{K_2 q_e^2 e^t}{1 + K_2 q_e t} \quad (7)$$

where k_2 is pseudo-second-order rate constant.

The equation that defines the Elovich model is based on a kinetic principle that assumes that adsorption sites increase exponentially with adsorption; this implies multilayer adsorption. The linear forms of the Elovich model are expressed as follows:

$$\frac{q_e}{q_m} = K_E C_e e^{\frac{q_e}{q_m}} \quad (8)$$

but the linear form is expressed as follows:

$$\ln \frac{q_e}{q_e} = \ln K_E q_m - \frac{q_e}{q_m} \quad (9)$$

Elovich maximum adsorption capacity and Elovich constant can be calculated from the slope and intercept of the plot of $\ln(q_e/C_e)$ versus q_e .

For the Weber-Morris Kinetic and Intra-particle diffusion model the fractional uptake of the solute on the particle, F , in a liquid-solid system will vary with the function:

$$\frac{D_0 t^{0.5}}{r^2} \quad (10)$$

Hence there is a linear relationship between F and $t^{0.5}$ for much of the adsorption process. F can be defined as:

$$F = \frac{(C_0 - C_t)}{C_0} \quad (11)$$

The Intra-particle diffusion parameter, k_i , can be defined as the linear gradient of a graph of the amount of contaminant adsorbed per gram of adsorbent (q_t) against the square root of time, $t^{0.5}$. Hence the diffusion rate parameter, k_i , is evaluated from:

$$k_i = \frac{1}{t^{0.5}} q_t \quad (12)$$

Rearranging Eq. (12),

$$q_t = k_i t^{0.5} \quad (13)$$

2.5 Adsorption Isotherm Studies

Different concentrations (20, 30, 40, and 50mg/L) of Brilliant Green Dye were prepared. 0.09g of the adsorbent was introduced into each of the solvent concentrations and agitated at 100rpm, constant pH, and temperatures at 30, 40, and 50°C, the isotherm adsorption studies were studied. After 180 minutes, the solution was filtered and the concentration of the supernatant solution was taken using a visible spectrophotometer thus ascertaining the amount of dye ions adsorbed. The amount of dye adsorbed the K-CF was calculated from the equation (1). The adsorption isotherms of the processes were studied using model equations, such as Langmuir, Freundlich, Temkin, and Halsey equations. Langmuir isotherm accounts for the surface coverage by balancing the relative rates of adsorption and desorption (dynamic equilibrium). The linear forms of the Langmuir model are as shown in equation (14) (Ahmadipouya et al., 2021):

$$\frac{C_e}{q_e} = \frac{1}{q_{max} K_L} + \frac{C_e}{q_{max}} \quad (14)$$

In which, q_{\max} is the theoretical maximum adsorption capacity (mg/ g) when dye molecules cover a uniform monolayer on the surface. K_L (L/ mg) is the Langmuir coefficient that is related to the affinity of the binding site i.e. adsorption energy. Freundlich model, assumes the multilayer coverage of adsorbate onto the heterogeneous adsorbent surface, though adsorption capacity was dependent on the equilibrium. The linear forms of the Freundlich model are as shown in equation (15):

$$\ln q_e = \ln K_F + \frac{1}{n_F} \ln C_e \quad (15)$$

“ K_F and n_F are Freundlich constants, related to the capacity and strength of adsorption, respectively. $1/n_F$ is related to the extent of adsorbent surface heterogeneity. The Temkin isotherm interplays between the adsorbent and the adsorbate and assumes that the absorbed heat decreases linearly with the surface coating, which is the reason for the adsorbent-adsorbate interaction. The linear equation of the Temkin isotherm is expressed according to equation (16)” (Feng et al., 2021):

$$q_e = B_1 \ln K_T + B_1 \ln C_e \quad (16)$$

In this equation, B_1 (RT/b) is the Temkin constant, which represents the heat of absorption, and K_T is relevant to the maximum energy band (L/mg). The adsorption isotherm can be given as follows:

$$\ln q_e = \frac{1}{n_H} \ln K_H - \frac{1}{n_H} \ln C_{qe} \quad (17)$$

where K_H and n are Halsey isotherm constant and they can be obtained from the slope and intercept of the plot of $\ln q_e$ versus $\ln C_e$.

2.6. Adsorption Thermodynamics

To properly describe the changes during the sorption processes and to rightfully conclude on the nature of the reactions, thermodynamic adsorption parameters such as ΔG° , ΔH° , and ΔS° will be investigated using equations (18) to (23).

$$\ln X_m = \frac{-\Delta H}{T} + K \quad (18)$$

$$\ln K_e = \ln A - \frac{E_a}{RT} \quad (19)$$

Where $\ln X_m$ is the natural logarithm for the greatest amount adsorbed (mg/g), K is the constant of Van't Hoff equation, R is the universal gas constant ($8.314 \cdot 10^{-3} \text{ J/mol} \cdot \text{K}^{-1}$) and T is the temperature in Kelvin.

$$\Delta G^\circ = -RT \ln K \quad (20)$$

where $K = \frac{Q_e \times m}{C_e \times V}$

$$\Delta G^\circ = \Delta H - T \Delta S^\circ \quad (21)$$

$$\Delta S^\circ = \frac{\Delta H - \Delta G^\circ}{T} \quad (22)$$

Combining equations 20 and 21 gives equation 23.

$$\ln K_a = \left(\frac{\Delta S^\circ}{R} \right) - \left(\frac{\Delta H^\circ}{RT} \right) \quad (23)$$

where K_a is the dependency of the equilibrium association constant ($K_a = b$, from Langmuir constant, L/mol), and R is the universal gas constant ($8.314 \text{ J mol}^{-1} \text{ K}^{-1}$). It is well known that the unit for ΔG° is J mol^{-1} . Since the unit for the term RT is also J mol^{-1} , the equilibrium constant K in Eq. (20) must be dimensionless (Okoye, Onukwuli, and Okey-Onyesolu, 2017), and T is the solution temperature.

3. RESULTS AND DISCUSSION

3.1 Batch Adsorption Studies of the Operating Variables on the Adsorbent

3.1.1 Effect of pH

The pH is a very important parameter in sorption experiments. The adsorption capacity was greatly influenced by the surface load and ionization degree of the adsorbate functional groups. The influence of pH on BGD was performed in the range of pH 2 to 10 for the adsorbent dose = 0.03g, temperature = 40°C, and initial dye concentration = 30 mg/L as shown in Fig.2. The optimum pH was observed to be at pH 8. The removal percentage increased from 55.3 to 87.6 for the adsorbent as the pH changed from acidic to basic. The reason for this behavior is that BGD is a cationic dye that stays positively charged in solution. "As the solution pH increases, more sorption sites (negatively charged) become available. These sites form an electrostatic attraction

with dye molecules, thus the removal percentage increases indicating that the chemical reaction between dye molecules and negatively charged ions, affects the sorption process” (Guo et al., 2014).

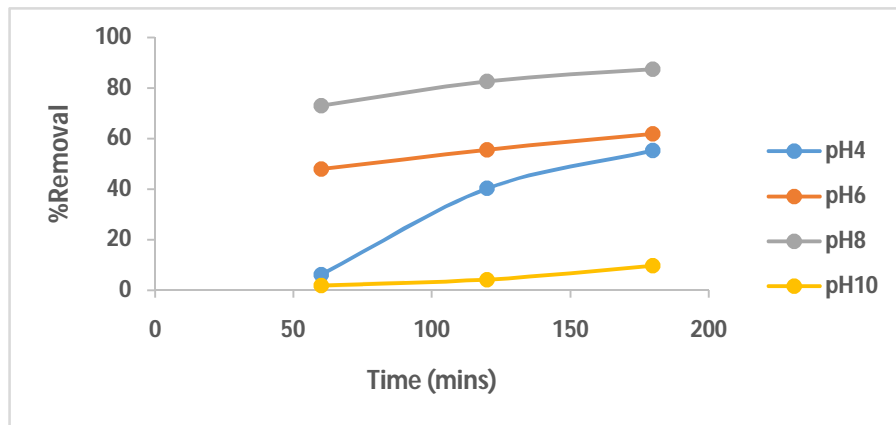


Fig.2 Influence of initial pH in terms of contact time at various pH on the adsorption efficiency of BGD at the concentration of 30 mg/l, and for 180 min using K-CF with a dose of 0.03 g/20 ml.

3.1.2 Effect of Adsorbent Dosage

The optimal dose of the adsorbent is also important in sorption studies as this study was made to discover the adsorption capacity with a minimum dose of an adsorbent. Tests were performed with varying adsorbent doses on the scale of (0.03 – 0.15) g/20ml with the initial dye concentration = 30 mg/L, pH = 8, and temperature 40°C for K-CF. Fig.3 shows that for K-CF, the optimum dose was 0.09g/20ml beyond which the adsorption capacity reduces because of excessive loading of the adsorbent.

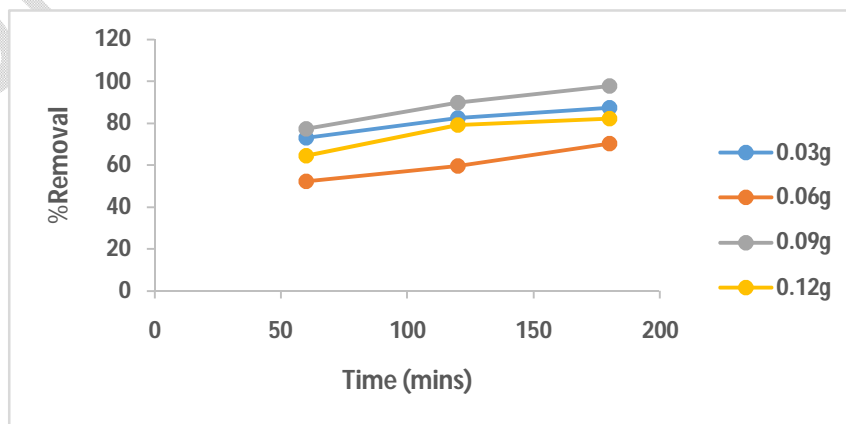


Fig.3, Influence of adsorbent dosage in terms of contact time at various dosages on the adsorption efficiency of BGD at a concentration of 30 mg/l, and for 180 min using K-CF at pH 8.

3.1.3 Effects of contact time and initial concentration

The influence of contact time is necessary for the design of any batch experiment. From the experimental results, it was found that more than 80% of the dye was adsorbed during the first 120 min. It gradually began to slow towards equilibrium in 180 min. Initially, the adsorption rate was fast as the outer surface of the sorbent which had a huge number of available sites for adsorption. Gradually dye molecules penetrate the adsorbent's inner pores and the adsorption rate decreases gradually (Mohammadi et al., 2017). Fig.4 shows the impact of BGD adsorption using K-CF with initial concentrations of 20, 30, 40, and 50 mg/L at pH = 8 adsorbent dose = 0.03 g/20ml, and temperature = 40°C. The dye removal rates decreased as the concentration of BGD raised from 20 to 50 mg/20ml, on the other hand, the adsorption capacity enhanced from 0.6 to 19.2mg/g. This is because the adsorbents have a finite number of active binding sites.

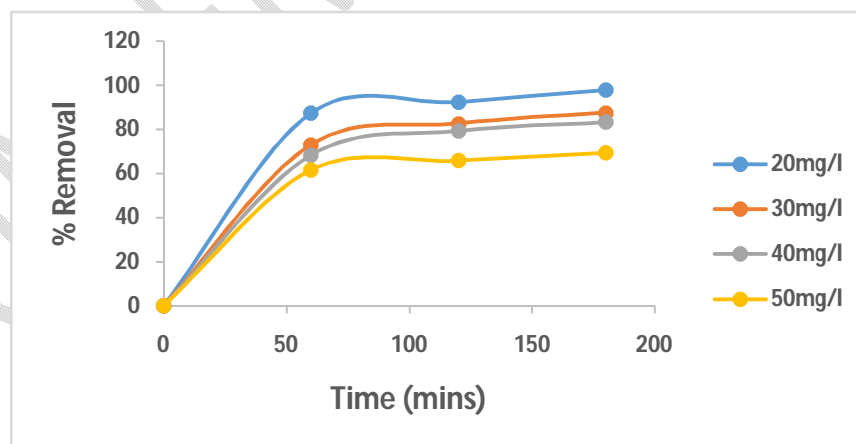


Fig. 4 Influence of BGD concentrations in terms of contact time on the adsorption efficiency of BGD, with 0.03g/20ml adsorbent for 180 min at pH 8 at 40°C; and K-CF with 0.09g/20ml for 180mins at pH 8.

3.2 Adsorption Kinetic Studies

The kinetic data were collected experimentally by mixing 40mg/l BGD solutions at different contact times (10–210 min) with a constant K-CF dose of 0.09g/l, at temperatures of 30, 40, and 50°C. To investigate the kinetic models, pseudo-first-order, pseudo-second-order, Elovich, and intra-particle diffusion models were used. The kinetic parameters and correlation coefficient (R^2) are listed in Table 1 as extracted from the kinetic plots from Figures 5 to 8. The pseudo-second-order model fitted the experimental data better with correlation coefficient (R^2) 0.97, 0.995, and 0.99 at the three different temperatures for the adsorbent K-CF, and the calculated q_e was close to the experimental data in the pseudo-second-order model thereby validating the model. Hence, the pseudo-second-order model described the kinetic data more accurately than other kinetic models. Also, from Table 1, there is a constant increase in rate constant in the pseudo-second-order model as the temperature increases.

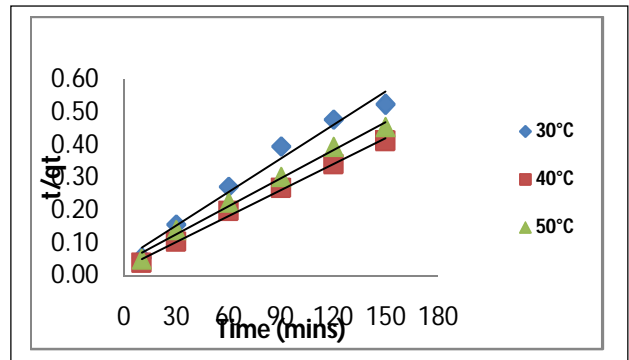
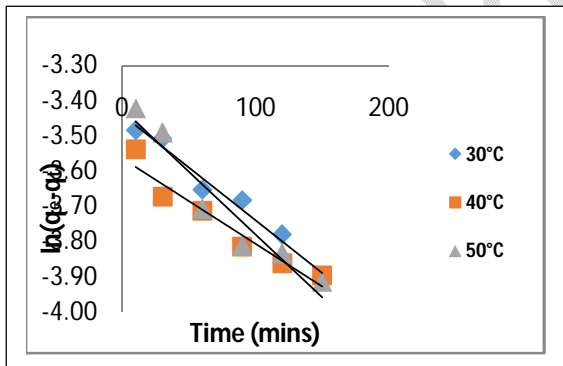


Fig. 5 Linearized Pseudo-First-Order plot for BGD on K-CF Fig. 6 Linearized Pseudo-Second Order plot on K-CF for BGD on K-CF

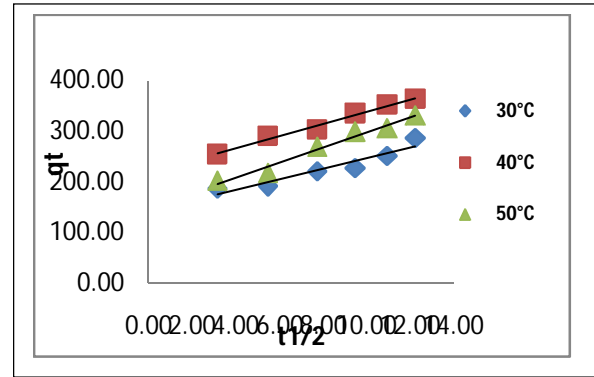
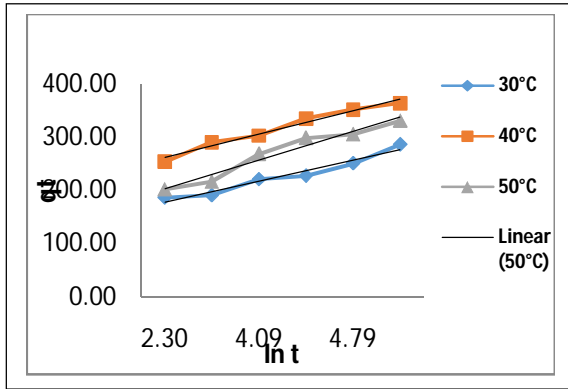


Fig. 7 Linearized Elovich plot for BGD on K-CF Fig. 8 Linearized Intra-particle plot for BGD on K-CF

Table 1 Adsorption Kinetic Parameters of BGD on K-CF at Concentration of 40mg/l and at Different Temperatures

Adsorbent C_0 (mg/l)	PFO Model				PSO Model			Elovich Model			Intra Particle Diffusion Model		
	q_e exp (mg/g)	q_e Cal (mg/g)	K_1	R^2	q_e Cal (mg/g)	K_2	R^2	Intercept	K_e	R^2	Diffusion Intercept	K_i	R^2
40	7.4	0.0284	0.024	0.9354	40.65	0.2328	0.9953	240.3	0.0457	0.9724	218.52	12.022	0.9845
303	5.7	0.0321	0.03	0.974	19.49	0.774	0.9738	158.74	0.051	0.95	141.94	10.449	0.9027
313	7.4	0.0284	0.024	0.9354	40.65	0.2328	0.9953	240.3	0.0457	0.9724	218.52	12.022	0.9845
323	6.6	0.0326	0.036	0.9264	24.1	0.6151	0.9913	176.44	0.0372	0.9534	149.21	14.836	0.9722

3.3 Adsorption Isotherm

Equilibrium adsorption isotherm is very useful for the analysis and design of adsorption systems. The equilibrium adsorption experiments were carried out by batch process for different initial BGD concentrations (20 to 50 mg/L) at 30°C, 40°C, and 50°C. The adsorption experimental data were plotted for linear isotherm models as shown in figures K-CF, and various isotherm constants were calculated as shown in Table 2. The equilibrium adsorption data were analyzed by Langmuir, Freundlich, Temkin, and Halsey isotherm models. The correlation coefficients (R^2) showed that the obtained equilibrium data for the three temperatures were better fitted to the Langmuir isotherm model than the Freundlich, Temkin, and Halsey isotherm models.

The maximum adsorption values calculated from the Langmuir isotherm model were 81.3, 65.36, and 454.55 mg/g at 30°C, 40°C, and 50°C respectively. The essential characteristic of the dimensionless separation factor (RL) values calculated as Equation (2.14) were in the range of 0.084 – 0.132, 0.052 – 0.121 and 0.339 – 0.562 at 20, 30, and 40°C. The values of $0 < RL < 1$ indicated that the adsorption of brilliant green was favorable at all temperatures as observed in the results.

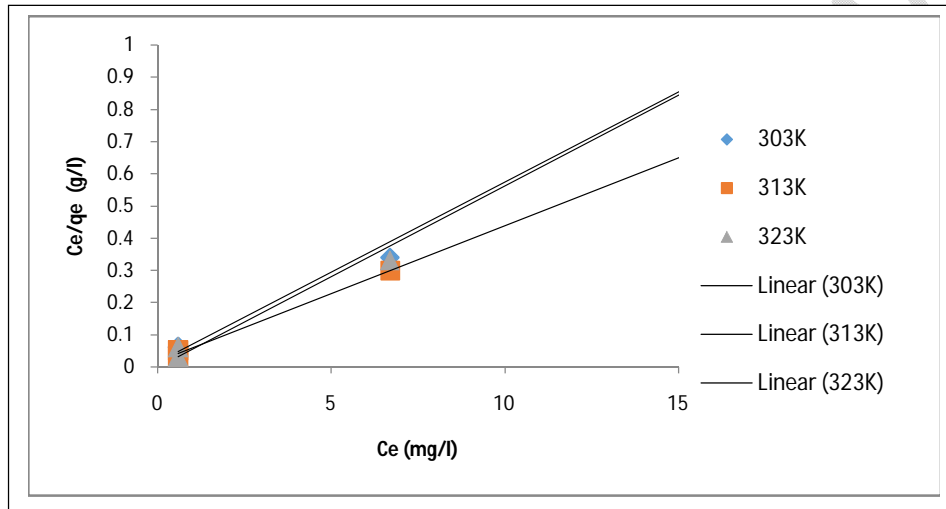


Fig. 9 Linearized Langmuir isotherm plot for the adsorption of BGD on K-CF

The Freundlich isotherm model is an empirical model that describes adsorption with heterogeneous surface. As shown in Table 2 the value for $1/n$ below 1 indicated a normal Freundlich isotherm model and reflected the favorable adsorption (Laskar and Kumar, 2018).

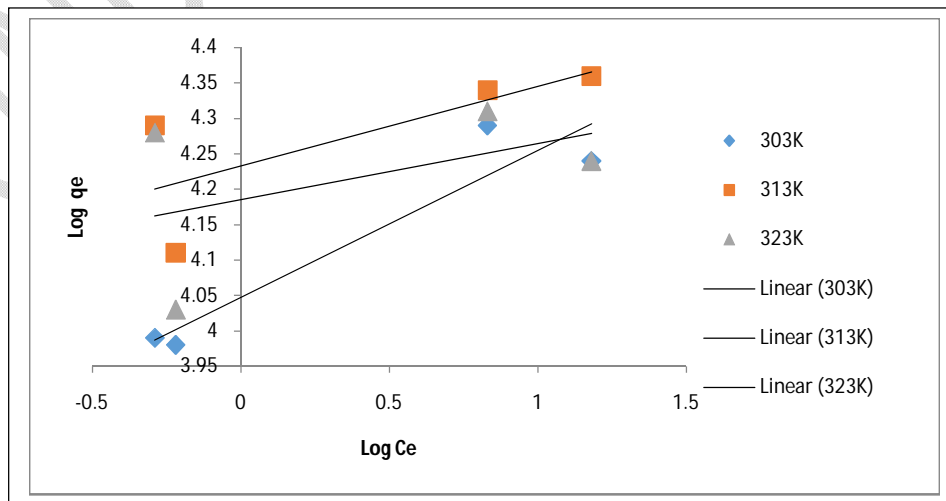


Fig.10 Linearized Freundlich isotherm plot for the adsorption of BGD on K-CF.

In Table .2, the Temkin constant, A_T , can be considered a sort of adsorption potential for dye adsorption and the calculated values were 1.02 and 1.007 L/g at 20, 30, and 40°C, respectively. The b_T values, related to the heat of adsorption, were 1.19, 1.17 and 2.11 KJ/mol, suggesting a strong interaction between BGD molecules and K-CF (Daneshvar et al.,2014).

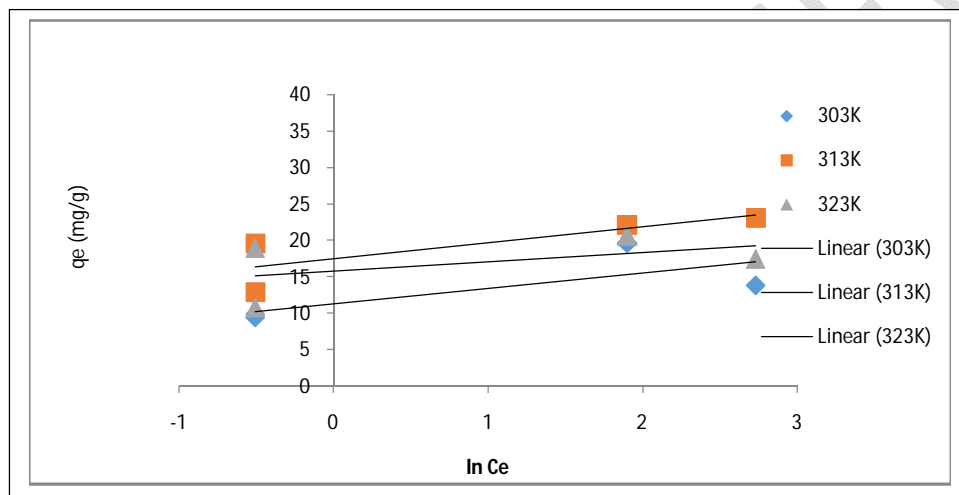


Fig. 11 Linearized Temkin isotherm plot for the adsorption of BGD on K-CF

Figure 12 give the Halsey isotherm model of BGD on K-CF. The Halsey isotherm parameters calculated and tabulated in Table 2 showed that the R^2 values for the K-CF at the temperature variations of 30□, 40□ and 50□ were 0.998, 0.452 and 0.366 respectively with best R^2 value at 30□.

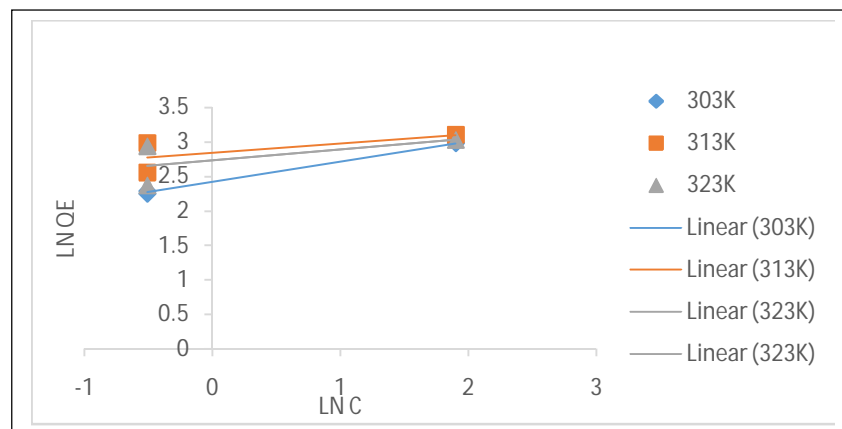


Fig. 12 Linearized Halsey isotherm plot for the adsorption of BGD on K-CF

Table 2 Isotherm parameters of brilliant green dye adsorption by K-CF at different temperatures of 30, 40, and 50 °C (pH = 8, K-CF dose = 0.09g, contact time = 180 min).

Isotherms	K-CF		
	30 °C	40 °C	50 °C
Langmuir Isotherm (mg/g)			
q_{max} (mg/g)	81.3	65.36	454.55
K_L (L/mg)	0.22	0.36	0.04
R_L	0.0836 - 0.1319	0.0523 - 0.1212	0.3390 - 0.5618
R^2	0.993	0.999	0.993
Freundlich Isotherm			
K_F (L/g)	2.271	2.132	2.226
$1/n$	0.498	0.523	0.474
R^2	0.991	0.996	0.993
Temkin Isotherm			
$B = R_T/B_t$	2.11	2.22	1.27
b_T (KJ/mol)	1.193	1.173	2.113
A (L/g)	1.01	1.02	1.007
R^2	0.559	0.644	0.239
Halsey Isotherm			
K_H	3.7×10^3	1.02×10^9	4.3×10^7
n_H	3.394	7.304	6.427
R^2	0.998	0.452	0.366

3.4 Adsorption Thermodynamics Parameters

The adsorption thermodynamics parameters of BGD by K-CF were studied at different temperatures (30°C, 40°C, and 50°C). The equilibrium adsorption constant ($K=q_e/C_e$) obtained at each temperature for the adsorbent was used for determining the free energy of adsorption (ΔG). At the initial optimal BGD concentration of 20mg/l, the ΔG values at 30°C, 40°C, and 50°C were presented in Table 3. Then, ΔH and ΔS were determined from the intercept and slope of the straight line, respectively. ΔG values became more negative with increasing temperature, supporting that adsorption was favored with increasing temperature. The negative value of ΔG indicated the feasibility of the process and the spontaneous nature of the adsorption. The values of ΔH and ΔS were also represented on the table.

Table 3 Thermodynamics Functions ΔG° , ΔS° and ΔH° of BGD adsorbed on K-CF

BGD Concentration		20Mg/l				
T(K)	1/T(T-1)	Ln Kd = ln(qe/Ce)	Kd	ΔH° (KJ/mol)	ΔS° (KJ/K.mol)	ΔG° (KJ/mol)
303	0.0033	1.335	3.8			-1,227,616
313	0.0032	2.512	12.33	-11.508	4051.5	-1,268,131
323	0.0031	0.5247	1.69			-1,308,646

4. Conclusion

This study investigated the novel synthesis of Keratin-Chicken feathers (K-CF) for removal of Brilliant Green Dye (BGD) as a contaminant in a textile wastewater. The adsorbent was prepared using combined chemical and thermal activation methods, which enhanced its adsorption capacity. The percentage removal of the BGD was optimal at pH 8. Also, the percentage removal was optimal at 0.09g/20ml at the temperature of 40°C. It was investigated that the percentage of dye adsorbed was highest at the first 120mins. For the kinetic models, pseudo-second-order model fitted the experimental data better than the other models used, while the Langmuir isotherm model was best fitted for different initial BGD concentrations (20 to 50 mg/L) at 30°C, 40°C, and 50°C. The negative value of ΔG indicated the feasibility of the process and the spontaneous nature of the adsorption process using the adsorbent from the thermodynamic study.

Disclaimer (Artificial intelligence)

Option 1:

Author(s) hereby declare that NO generative AI technologies such as Large Language Models (ChatGPT, COPILOT, etc) and text-to-image generators have been used during writing or editing of manuscripts.

Option 2:

Author(s) hereby declare that generative AI technologies such as Large Language Models, etc have been used during writing or editing of manuscripts. This explanation will include list the name, version, model, and source of the generative AI technology and as well as the all input prompts provided to a generative AI technology

Details of the AI usage are given below:

- 1.
- 2.
- 3.

References

1. Alvarez-Castillo, E., Felix, M., Bengoechea, C., & Guerrero, A. (2021). Proteins from Agri-Food Industrial Biowastes or Co-Products and Their Applications as Green Materials. *Foods*, 10(5). doi:10.3390/foods10050981.
2. Bellir, K., Bencheikh, M., Meniai, A., 2010. Removal of methylene blue from aqueous solutions
3. using acid activated Algerian bentonite: equilibrium and kinetic study. *International*
4. *Renewable Energy Congress*, Tunisia. Nov 5–7.
5. Bharathi, K.S., Ramesh, S.T., 2013. Removal of dyes using agricultural waste as low-cost adsorbents: a review. *Appl Water Sci* 3, 773–790. <https://doi.org/10.1007/s13201-013-0117-y>.
6. Chaitanya Reddy, C., Khilji, I. A., Gupta, A., Bhuyar, P., Mahmood, S., Saeed Al-Japairai, K. A., & Chua, G. K. 111 (2021). Valorization of keratin waste biomass and its

potential applications. *Journal of Water Process Engineering*, 40, 101707. doi:10.1016/j.jwpe.2020.101707

7. Chilakamarry, C. R., Mahmood, S., Saffe, S., Bin Arifin, M. A., Gupta, A., Sikkandar, M. Y., Begum, S. S., & Narasaiah, B. (2021). Extraction and application of keratin from natural resources: a review. *3 Biotech*, 11(5). doi:10.1007/s13205-021-02734-7
8. Daneshvar, E., M.S. Sohrabi, M. Kousha, A. Bhatnagar, B. Aliakbarian, A. Converti, and A-C. Norrström. 2014. Shrimp shell as an efficient bio adsorbent for Acid Blue 25 dye removal from aqueous solution. *Journal of the Taiwan Institute of Chemical Engineers*. 45(6): 2926-2934. doi: 10.1016/j.jtice.2014.09.019.
9. Duan, Y., Awasthi, S. K., Liu, T., Pandey, A., Zhang, Z., Kumar, S., & Awasthi, M. K. (2020). Succession of keratin-degrading bacteria and associated health risks during pig manure composting. *Journal of Cleaner Production*, 258, 120624.
10. Etim, U.J., Umoren, S.A., Eduok, U.M., 2016. Coconut coir dust as a low-cost adsorbent for the removal of cationic dye from an aqueous solution. *J. Saudi Chemical Society* 20, 67–76. <https://doi.org/10.1016/j.jscs.2012.09.014>.
11. Giteru, S. G., Ramsey, D. H., Hou, Y. K., Cong, L., Mohan, A., & Bekhit, A. (2023). Wool keratin as a novel alternative protein: A comprehensive review of extraction, purification, nutrition, safety, and food applications. *Comprehensive Reviews in Food Science and Food Safety*, 22(1), 643-687. doi:10.1111/1541-4337.13087.
12. Guo X., C. Kang, H. Huang, Y. Chang, C. Zhong, (2019). Microporous Mesoporous Mater 286.
13. Gupta, V.K., Suhas, I. Tyagi, Agarwal, S., Singh, R., Chaudhary, M., Harit, A., Kushwaha, S., 2016. Column operation studies for the removal of dyes and phenols using a low-cost adsorbent. *Global J. Environ. Sci. Manage.* 2, 1–10. <https://doi.org/10.7508/gjesm.2016.01.001>.
14. Khan N.A, Z. Hasan, S.H. Jhung (2021). Adsorptive removal of hazardous materials using metal-organic frameworks (MOFs): A review, *Journal of Hazardous Materials*.
 - a. luminescence and photocatalytic properties. *J Mol Struct* 1080: 44-51.
 - b. M.X., and Xu, P., 2020. Synergistic Removal of Copper and Tetracycline from Aqueous

15. Mane, V.S., Babu, P.V.V., 2011. Studies on the adsorption of Brilliant Green dye from aqueous solution onto low-cost NaOH-treated sawdust. *Desalination* 273, 321–329. <https://doi.org/10.1016/j.desal.2011.01.049>.
16. Mohammadi A.A., A. Alinejad, B. Kamarehie, S. Javan, A. Ghaderpoury, M. Ahmadpour, M.
17. Mondal, P.; Baksi, S.; Bose, D., 2017. Study of environmental issues in textile industries and recent wastewater treatment technology. *World Sci. News* 2017, 61, 98–109
18. N. Laskar, U. Kumar, 2018. Removal of Brilliant Green dye from water by modified BambusaTulda: adsorption isotherm, kinetics and thermodynamics study. *Int J. Environmental Science and Technology*. doi:10.1007/s13762-018-1760-5.
19. Nekouei, F., Nekouei, S., Tyagi, I., Gupta, V.K., 2015. Kinetic, thermodynamic, and isotherm studies for acid blue 129 removal from liquids using copper oxide nanoparticle-modified activated carbon as a novel adsorbent. *J Mol Liq* 201, 124–133. <https://doi.org/10.1016/j.molliq.2014.09.027>.
20. Nianxiang Hu, Jiang Liao, Xueliang Liu, Jinlong Wei, Li Wang, Min Li, Naixuan Zong, Ruidong Xu, Linjing Yang and Junli Wang. 2022. CNTs support 2D NiMOF nanosheets for asymmetric supercapacitors with high energy density. PMID: 36226657, DOI: [10.1039/d2dt02055f](https://doi.org/10.1039/d2dt02055f).
21. Okoye, C.C., Onukwuli, O.D., Okey-Onyesolu, C.F., Nwokedi, I.C., 2016. Adsorptive removal of Erythrosin B dye onto Terminalia Catappa endocarp prepared activated carbon: kinetics, isotherm, and thermodynamics studies. *Chem. Process Eng. Res.* 43, 26–43.
22. Onu, C.E., Oguanobi, N.C., Okonkwo, C.O., Nnamdi-Bejie, J., 2020a. Application of modified agricultural waste in the adsorption of bromocresol green dye. *Asian J. Chem. Sci.* 7 (1), 15–24. <https://doi.org/10.9734/ajocs/2020/v7i119011>.
23. Ossai, I. C., Hamid, F. S., & Hassan, A. (2022). Valorisation of keratinous wastes: A sustainable approach towards a circular economy. *Waste Management*, 151, 81-104. doi:10.1016/j.wasman.2022.07.021.
24. Perța-Crișan, S., Ursachi, C., Gavrițaș, S., Oancea, F., & Munteanu, F. D. (2021). Closing the Loop with Keratin-Rich Fibrous Materials. *Polymers (Basel)*, 13(11). doi:10.3390/polym13111896.

25. Saleh, T.A., Gupta, V.K., 2011. Functionalization of tungsten oxide into MWCNT and its application for sunlight-induced degradation of rhodamine B. *J Colloid Interface Sci* 362, 337–344. <https://doi.org/10.1016/j.jcis.2011.06.081>.
26. Saravanan, R., Gupta, V.K., Mosquera, E., Gracia, F., 2014a. Preparation and characterization of V₂O₅/ZnO nanocomposite system for photocatalytic application. *J Mol Liq* 198, 409–412. <https://doi.org/10.1016/j.molliq.2014.07.030>.
27. Salman Ahmadipouya, Mahdi Heidarian, Haris, Farhad Ahmadijokani, Atefeh Jarahiyan, Hossein Molavi, Firouz Matloubi Moghaddam, Mashallah Rezakazemi, 2021. Magnetic Fe₃O₄@ UiO-66 nanocomposite for rapid adsorption of organic dyes from aqueous solution. *J. Mol. Liq.* 322, 114910.
28. Tavlieva, M. P., S. D. Genieva, V. G. Georgieva, and L. T. Vlaev. 2013. Kinetic study of brilliant green adsorption from aqueous solution onto white rice husk ash. *Journal of Colloid and Interface Science*. 409: 112-122. doi: 10.1016/j.jcis.2013.07.052.
29. Tinoco, A., Rodrigues, R. M., Machado, R., Pereira, R. N., Cavaco-Paulo, A., & Ribeiro, A. (2020). Ohmic heating as an innovative approach for the production of keratin films. *Int J Biol Macromol*, 150, 671-680. doi:10.1016/j.ijbiomac.2020.02.122
30. Victor Alexandru Faraon, Eliza Gabriela Mihăilă, Naomi Tritcan, Bogdan Trică, Luiza Capră, Mihail-Bogdan Roman, Diana Constantinescu-Aruxandei, Florin Oancea, 2023. Keratin Extraction From Chicken Feathers In Aqueous Solutions
31. Wang CC, Jing HP, Wang P, Gao SJ (2015) Series metal-organic frameworks constructed from
- 1,10-phenanthroline and 3,3',4,4'-biphenyltetracarboxylic acid: Hydrothermal synthesis,
 - luminescence and photocatalytic properties. *J Mol Struct* 1080: 44-51.
32. Wang, R.Z., Huang, D.L., Liu, Y.G., Zhang, C., Lai, C., Wang, X., Zeng, G.M., Zhang, Q., Gong,
- M.X., and Xu, P., 2020. Synergistic Removal of Copper and Tetracycline from Aqueous
 - Solution by Steam Activated Bamboo Biochar, *J. Hazard. Mater.*, 384, 1-10.
33. Tasneem A, Sarker P, Uddin MK. Comparative Efficacy of Coagulation-Flocculation and Advanced Oxidation Process (AOP: Fenton) for Textile Wastewater Treatment. *Curr. J.*

Appl. Sci. Technol. [Internet]. 2020 Jun. 29 [cited 2024 May 31];39(17):41-5. Available from: <https://journalcjast.com/index.php/CJAST/article/view/2735>

34. Dada EO, Ojo IA, Alade AO, Afolabi TJ, Jimoh MO, Dauda MO. Biosorption of Bromo-based Dyes from Wastewater Using Low-Cost Adsorbents: A Review. J. Sci. Res. Rep. [Internet]. 2020 Sep. 30 [cited 2024 May 31];26(8):34-56. Available from: <https://journaljsrr.com/index.php/JSRR/article/view/1176>
35. Solayman HM, Hossen MA, Abd Aziz A, Yahya NY, Leong KH, Sim LC, Monir MU, Zoh KD. Performance evaluation of dye wastewater treatment technologies: A review. Journal of Environmental Chemical Engineering. 2023 Jun 1;11(3):109610.

UNDER PEER REVIEW